

Military Technical College
Kobry Elkobbah,
Cairo, Egypt



8th International Conference
on Aerospace Sciences &
Aviation Technology

MODELING OF GAS TURBINE BLADES SUBJECTED TO HIGH TEMPERATURE FLUID STREAMS

A.A. MOSTAFA*, M.A. MEHANNA**, M.S. FARID**, S.S. KOUSSA*

ABSTRACT

This paper presents the first phase of numerical modeling of a gas turbine blade subjected to a high temperature flow stream. Continuity, momentum, and energy equations along with high Reynolds number $k-\epsilon$ turbulence model were solved using a finite-element numerical computer program (ANSYS 5.3). Temperature and velocity fields were presented at different Reynolds numbers for a turbine blade airfoil and compared with the available experimental results. Results from flow computations around the turbine blade were used as a third kind boundary conditions for a coupled field thermal-structure analysis. The thermal stress due to the computed temperature distribution was obtained throughout the turbine blade airfoil with and without convection cooling configuration, the turbine blade service life, combined, thermal fatigue-creep failure mode, was predicted using strain ranges partitioning method. A Sun workstation was used to get a numerical solution of the governing equations. The numerical model provide quite detailed information that help in understanding the physics of the problem. The results showed good agreement with the experimental data available in the literature. The present numerical investigation presents an efficient and more economical technique, which has a great influence on the concurrent engineering concept.

KEY WORDS

Turbine blade, fluid flow, heat transfer, stress distribution, life prediction

* Mechanical Power Department, Cairo University, Giza, Egypt
** Egyptian Armed Forces, Cairo, Egypt

NOMENCLATURE

| | | | |
|----------|----------------------------------------------|--------------------|----------------------------------------------------------|
| C | = blade chord length | T_c | = coolant air temperature |
| C_μ | = constant | T_g | = hot gas temperature |
| D | = cooling hole diameter | T_m | = metal temperature |
| E | = law of the wall constant | U_c | = coolant flow velocity |
| h | = heat transfer coefficient | y^* | = dimensionless thickness |
| K | = effective conductivity | ε_{cp} | = strain for creep in tension, fatigue in compression |
| k | = law of the wall constant | | = generalized flow variables |
| N_{cp} | = cycles corresponding to ε_{cp} | ρ | = density |
| n | = blades number in stage | τ_w | = wall shear stress |
| P_r | = Prandtl number | | |
| Re | = Reynolds number | | |

INTRODUCTION

Gas turbines are expected to run for thousands of hours without major overhauls. It follows that they can't be based upon aerodynamic considerations alone. Successful design results only from a highly iterative series of thoughtful aerodynamics, heat transfer, materials and structural evaluations. The best solution for each design problem involved with the gas turbine is effectively couples the important factors together in the correct proportions.

One of the most critical parts of the gas turbine is the turbine blade. The word critical here is not only concerned with the functionality of these blades, but also with its severe environmental and operating conditions, which in turn imply complications in its design and analysis. The problem of turbine blade analysis is highly coupled one. It involves CFD, thermal, structural coupling. Starting with CFD analysis, heat transfer coefficient is determined over the blade boundaries. The calculated heat transfer coefficient is then used as a third type boundary condition for the thermal-structural coupled field analysis. Temperature and stress distribution is determined and used with assumed blade material characteristics for calculating the turbine lifetime.

Fairly rare works were concerned with integrated turbine blade analysis, although a quite large number of literatures are found in each field. An example of this is the work done by Mehanna [1]. CFD-thermal-structural analysis was used for calculations of lifetime required for crack initiation of the turbine blade. A suggested convective cooling technique was optimized to maximize the lifetime.

The NASA HOST "Hot Section Technology" [2] has focused on providing methods for solving and analyzing problems incorporated with components,

which operates under severe environmental conditions. An integration of prior developed codes covering different analysis aspects was made.

Edhin and Chanis [3] used the conservation laws for energy, mass and momentum to derive multidisciplinary-coupled finite element involving fluid mechanics, heat transfer and nonlinear theories of solid mechanics. Interactions among stated disciplines are represented by both domain and boundary coupling and a four-node quadrilateral coupled finite elements were used with iterative solution procedure.

FLUID FLOW MODEL

A highly loaded, low solidity turbine blade airfoil was selected for analysis, taking into consideration the availability of extensive test data in the literature. The first turbine blade airfoil is that one used by Daniels and Browne [4]. The airfoil has some noticeable characteristics. It is thick, highly cambered and stuffy which means that, it will exhibit a wide variety of fluid phenomena and are not especially susceptible to classical approaches.

Flow Governing Equations

Continuity Equation

From the law of mass conservation comes the continuity equation:

$$\frac{\partial(\rho V_x)}{\partial x} + \frac{\partial(\rho V_y)}{\partial y} = 0 \quad (1)$$

Momentum Equation

It is a force equilibrium in both directions x and y

$$\frac{\partial(\rho V_x V_x)}{\partial x} + \frac{\partial(\rho V_y V_x)}{\partial y} = -\frac{\partial P}{\partial x} + \frac{\partial}{\partial x} \left(\mu_e \frac{\partial V_x}{\partial x} \right) + \frac{\partial}{\partial y} \left(\mu_e \frac{\partial V_x}{\partial y} \right) + T_x \quad (2)$$

$$\frac{\partial(\rho V_x V_y)}{\partial x} + \frac{\partial(\rho V_y V_y)}{\partial y} = -\frac{\partial P}{\partial y} + \frac{\partial}{\partial x} \left(\mu_e \frac{\partial V_y}{\partial x} \right) + \frac{\partial}{\partial y} \left(\mu_e \frac{\partial V_y}{\partial y} \right) + T_y \quad (3)$$

where

$$T_x = \frac{\partial}{\partial x} \left(\mu \frac{\partial V_x}{\partial x} \right) + \frac{\partial}{\partial y} \left(\mu \frac{\partial V_y}{\partial x} \right) \quad (4)$$

$$T_y = \frac{\partial}{\partial x} \left(\mu \frac{\partial V_x}{\partial y} \right) + \frac{\partial}{\partial y} \left(\mu \frac{\partial V_y}{\partial y} \right) \quad (5)$$

Energy Equation

Based on the law of conservation of energy and expressed in terms of the total (stagnation) temperature, the energy equation is:

$$\frac{\partial}{\partial x} (\rho v_x C_p T_0) + \frac{\partial}{\partial y} (\rho v_y C_p T_0) = \frac{\partial}{\partial x} \left(k \frac{\partial T_0}{\partial x} \right) + \frac{\partial}{\partial y} \left(k \frac{\partial T_0}{\partial y} \right) + w^v + e^k + q_v + \Phi \quad (6)$$

The static temperature is calculated from the total temperature by the equation:

$$T = T_0 + \frac{V^2}{2C_p} \quad (7)$$

The viscous work term is:

$$w^v = v_x \mu \left[\frac{\partial^2 v_x}{\partial x^2} + \frac{\partial^2 v_x}{\partial y^2} + \frac{\partial}{\partial x} \left(\frac{\partial v_x}{\partial x} + \frac{\partial v_y}{\partial y} \right) \right] + v_y \mu \left[\frac{\partial^2 v_y}{\partial x^2} + \frac{\partial^2 v_y}{\partial y^2} + \frac{\partial}{\partial y} \left(\frac{\partial v_x}{\partial x} + \frac{\partial v_y}{\partial y} \right) \right] \quad (8)$$

The viscous dissipation term is:

$$\Phi = 2\mu \left[\left(\frac{\partial v_x}{\partial x} \right)^2 + \left(\frac{\partial v_y}{\partial y} \right)^2 \right] + \mu \left[\left(\frac{\partial v_x}{\partial x} + \frac{\partial v_y}{\partial y} \right)^2 \right] \quad (9)$$

The kinetic energy term is:

$$e^k = -\frac{\partial}{\partial x} \left[\frac{K}{C_p} \frac{\partial}{\partial x} \left(\frac{1}{2} |v|^2 \right) \right] - \frac{\partial}{\partial y} \left[\frac{K}{C_p} \frac{\partial}{\partial y} \left(\frac{1}{2} |v|^2 \right) \right] \quad (10)$$

Turbine Blade and Cascade Geometry

The profile coordinates are listed in table (1) and the blade cascade geometry is illustrated in figure (1). The main cascade dimensions are summarized as follows:

| | | | |
|------------------------|-----------|-----------------------|-----------|
| Chord length | = 36.9 mm | Blade span | = 50 mm |
| Pitch-to-chord ratio | = 0.97 | Leading edge diameter | = 5 mm |
| Trailing edge diameter | = 2 mm | Throat dimension | = 14.1 mm |

Boundary Conditions

The inlet parameters is assumed to be uniformly distributed pitchwise direction

$$\begin{array}{ll} V_x & = 87 \text{ m/s} \\ \text{Temperature} & = 423 \text{ k} \end{array} \quad \begin{array}{ll} V_y & = 103 \text{ m/s} \\ \text{Turbulence level "Tu \%"} & = 0.04 \end{array}$$

Considering the inlet turbulence kinetic energy (K.E), it was calculated from [5]

$$K.E_{in} = 3/2 [(Tu\%) V]^2 \tag{11}$$

The rate of energy dissipation at the inlet section was obtained from [5]

$$\varepsilon = \frac{C_\mu(K.E)^{3/2}}{L} \tag{12}$$

where L is the characteristic length scale and $L = 0.01 L_1$, where L_1 is the pitch of the cascade

The involved blade is a part of turbine rotor or stator, then it is based on a surface of revolution. For N number of blades at certain stage, the flow is periodically symmetric, at angle $\theta = 360/N$, where N is the number of blades in each stage. The periodic boundary conditions are unknown but identical at the two boundaries as shown in figure (1), which can be expressed mathematically as:

$$\varphi(Z, R, \theta) = \varphi(Z, R, \theta + 360/N) \tag{13}$$

No slip condition is applied through wall function for the task of reducing the number of grid nodes near the wall. At nodes nearest to the solid walls, the velocity vector is assumed to be parallel to it. It is located on predetermined distance away from the wall. Along this distance the dimensionless velocity V^+ , assuming the following form [5]:

$$V^+ = \begin{cases} V / \sqrt{\frac{\tau_w}{\rho}} & \text{for } y^+ \leq 11.5 \\ (1/k) \ln(Ey^+) & \text{for } y^+ > 11.5 \end{cases} \tag{14}$$

$$\tag{15}$$

where The first node is located at nearly (0.005*C) from the wall and k, E are law of the wall constants [5].

Finite Element Model

Significant gradients are calculated near the inlet and outlet in the leading and trailing edge regions. This may cause an unbalance, so the problem domain

was extended to allow the flow to develop at least partially before inlet and exit boundaries as shown in figure 1. The periodic boundary position was calculated based on the pitch of the cascade. It represents the line of symmetry between two successive chord lines and based on real turbine stage data.

The used element is Fluid 141-referred to the ANSYS 5.3 element's library-has the following characteristics:

| | | |
|---------------------|---|---------------------------------------------------------------------------------------------------|
| Dimensions | : | 2-D |
| Shape | : | Quadrilateral "four nodes" and triangle "three nodes". |
| Degrees of freedom: | : | Fluid velocity, pressure, temperature, turbulent kinetic energy and turbulent dissipation energy. |
| Type | : | Isoparametric |

Negative values of absolute pressure and absolute static temperature have to be prevented as these would lead to a negative density. It was found that the best way to avoid this is by using of approximated converged solutions of laminar flow as input for the real case under consideration. The partially converged solution is used as input for turbulent with the real viscosity. The partially converged solution of turbulent incompressible flow is used as input for the turbulent compressible flow. Under-relaxation factors are used for the pressure and velocity parameters and released gradually as long as the solution is converged, since this will be on the use of time. Also relaxation factor are used for effective viscosity.

HEAT TRANSFER AND STRUCTURAL MODEL

The described airfoil geometry was used with convective cooling configuration. Three circular cooling holes are distributed over the blade material.

Convection boundary conditions, obtained from the solution of the fluid flow around the airfoil, are applied to the external boundaries of the airfoil. The mass flow of air required to accomplish the necessary cooling depends entirely upon the cooling configuration. If cooling effectiveness is defined as:

$$\Phi = \frac{T_g - T_m}{T_g - T_c} \quad (16)$$

The required average cooling effectiveness is the strongest parameter determining the method of cooling and the mass flow rate of cooling air. Convective cooling is used where the average cooling effectiveness levels required are less than about 0.5, this limitations exist due to the limited air

supply pressure and such higher effectiveness could be possible only with higher supply pressure. Also with higher effectiveness levels and convective cooling, the temperature gradients tend to become very large and thus causing thermal stress problem.

Using curves relating the cooling effectiveness to the cooling flow rate as shown in figure (2), the amount of coolant flow required to achieve the desired metal temperature of a turbine airfoil by means of convective cooling is provided

Knowing the mass flow rate of the whole stage, the mass flow rate for each blade is calculated as:

$$\dot{m}_{blade} = \frac{\dot{m}_{stage}}{N_b} \quad (17)$$

It is possible to calculate the mass flow rate distribution in each hole of the turbine blade as one-dimensional flow using electric network analogy, where

$$\dot{m}_{blade} = \sum_{i=1}^n r_i \dot{m}_i \quad (18)$$

$$i = 1, 2, \dots, n$$

where r_i is the cooling hole radius.

Reynolds number in each hole can be calculated as a function of mass flow rate

$$\dot{m} = \rho_c \frac{\pi}{4} D^2 u_c \quad (19)$$

From the above data, the heat transfer coefficient for constant surface temperature circular hole and turbulent flow is calculated from:

$$h = \frac{K}{\Delta} (0.021) \sqrt{Pr} R_e^{0.8} \quad (20)$$

Thermal stresses arise due to temperature gradients and restrained material displacement. The problem is assumed to be Plane State of stress where each node has two displacements in x and y directions.

$$u_x = u_y = 0 \quad (21)$$

The used element for solving the coupled structural and thermal problem is Plane 13, referred to ANSYS 5.3 element's library. It elements has the following characteristics:

Dimensions : 2-D

| | | |
|--------------------|---|--------------------------------------------------------|
| Shape | : | quadrilateral "four nodes" and triangle "three nodes". |
| Type | : | Isoparametric |
| Degrees of freedom | : | Temperature, displacement in x and Y direction. |

LIFE PREDICTION

Loading Cycle and Material Properties

The turbine blade is expected to experience a combined low cycle fatigue-creep failure mode. Figure (3) shows a real mission cycle in terms of turbine inlet temperature and engine speed. For adequacy, a simplified loading cycle is used as shown in figure (3) with dashed lines.

Single crystal Nickel based alloy Rene`80 with improved high temperature strength, fatigue and creep properties was used. Temperature dependent physical properties and cyclic stress-strain properties used in the analysis are that one extracted from extensive factory tests done by Mcknight et al. [6].

Strain Range Partitioning

Mcknight et al. [6] provided the equations for the four SRP life relations of Rene`80 measured at temperature 600 k. The simplified loading cycle is represented by a pure $\Delta\epsilon_{cp}$

$$\Delta\epsilon_{cp} = 11.8(N_{cp})^{-0.64} \quad (22)$$

RESULTS and DISCUSSIONS

CFD Results

The normalized heat flux and heat transfer coefficients for both suction and pressure surfaces are presented as a function of dimensionless chordwise distance as shown in figures (4) to (7). Assessment of the predicted results will rely on the comparison with the corresponding experimental data measured by Daniels and Browne [4]. Uncertainty in the experimental data is considered in the order of 10%. For more details about the experiment conditions, equipment, and procedures refer to Daniel and Browne [4]. They used different codes to achieve numerical results for the task of its assessment. These codes are the Cebeci-Smith referred to as (C-S), Patanker-Spalding or (P-S), Wilox "EDDY BL" or (W-E) and Wilox program with all turbulent parameters supplied or (W-T). These calculations are presented in figures (4) and (6).

Considering the suction surface, predictions achieved in the present work behave qualitatively in the same manner as the experimental results. High leading edge heat transfer rate, is followed by a rapid fall in the laminar section of the boundary layer. Sharp rise at the end of transition region, is followed by gradually falling of heat transfer rate towards the trailing edge. In general, the predictions of the present work agree with the experimental data over the laminar and turbulent regions. However, there are some discrepancies in the transition region (0.2 to 0.6 x/L).

Considering the pressure surface, boundary layer development is expected to be more complicated than suction surface as shown in figures (4) and (5). Transition region is not clearly evident at these flow conditions. Turbulent flow region is indicated by stabilized values of both heat transfer data at distance about 0.5 x/L . The values of heat transfer predictions over the laminar flow region on the pressure surface are greatly overestimated than the measured one. This can be attributed due to the use of high Reynolds number turbulence model.

Thermal and Structural Results

Results of thermal and structural calculations are presented in the form of contoured distribution over the blade material. Von Mises stress distribution is calculated with varying cooling temperature and heat transfer coefficients. The results of cooling temperature variations showed that it does not affect the general temperature distribution behavior, however it affects the localized region surrounding the cooling holes as shown in figures (8) and (9). Stress distribution shows that the trailing edge and leading edge are the most critical regions. These two regions generally characterized by high heating rates since they have high heat transfer coefficients. The trailing edge is the most difficult region to be cooled due to its small width and edge. Regions around the cooling holes are characterized by the lowest temperature values. The effect of heat transfer coefficient of coolant flow is found to be limited. It can be shown for the illustrated stress distributions that the cooling efficiency is very high in the thickness direction of the airfoil and that regions of high temperatures or low efficiency of cooling always exist in chordwise direction with respect to cooling holes position. In other words, a more efficient convective cooling is expected if cooling holes were allowed to be elongated in chordwise direction.

Life Prediction Results

Blade life is defined as the life time required for crack initiation in the blade material under combined low cycle fatigue-creep loading. It was calculated using strain range partitioning method. Blade life time was expected to increase

by decreasing the coolant flow temperature as the thermal stresses increase by decreasing the temperature difference. Trailing edge region was found to be the most critical region for which the crack initiation was expected to occur then propagate throughout the blade material.

CONCLUSIONS

- 1- Results of the present work have a very good agreement with the literature experimental results.
- 2- CFD analysis can be accelerated by proper selection of under-relaxation factors, also the selection of finite element number and size near the turbine blade wall is a critical criterion for obtaining convergence.
- 3- The most critical region from thermal stresses point of view was found to be the trailing edge region.
- 4- More efficient convective cooling can be obtained by allowing circular cooling holes to elongate in chordwise direction.

REFERENCES

- [1] Mehanna, M. A, "Aero-Thermo-Structural Analysis and Optimization of Gas Turbine Blades Using Finite Element Technique," Master thesis, Cairo university, 1999.
- [2] Mcknight, R. L, Cook, T. S, Bechtel, G. S, Huang, H. T, "Application of HOST Technology to the SSME HT-FTP Blade," Journal of Engineering for Gas Turbine and Power, Transactions of ASME, Vol. 113, 1991, pp. 140-144.
- [3] Edhin, E. S, Chanis, C. C, "Multidisciplinary Finite Elements for Coupled Analysis of Fluid Mechanics, Heat Transfer and Solid Mechanics," Structures, Structural Dynamics and Material Conference, AIAA, ASME, ASCE, AHS, Collection of Technical Papers, AIAA, 1995, pp. 1318-1327.
- [4] Daniels, L. D, W. B. Browne, W. B, "Calculation of Heat Transfer Rates to Gas Turbine Blades," Journal of Mass and Heat Transfer, vol. 24, no. 5, 1981, pp. 871-879.
- [5] T. Cebecci, A. M. Smith, "Analysis of Turbulent Boundary Layerm," Applied Mathematics and Mechanics, Vol. 15, Academic Press, New York, 1974.
- [6] Mcknight, R. L., J. H. Laflen, J. H., Halford, G. R., "Turbine Blade Nonlinear Structural and Life Analysis," Journal of Aircraft, Vol. 20, No. 5, 1983, pp. 475-480.

Table 1. Airfoil coordinates

| X | Y | X | Y |
|---------|--------|---------|---------|
| -36.694 | 33.561 | -00.368 | 00.5771 |
| -35.269 | 36.909 | -02.074 | 02.792 |
| -33.431 | 38.692 | -03.306 | 05.920 |
| -31.594 | 40.228 | -06.980 | 08.868 |
| -29.757 | 40.383 | -08.817 | 11.659 |
| -27.921 | 40.187 | -10.654 | 14.306 |
| 26.084 | 39.667 | -12.490 | 16.826 |
| -24.247 | 38.807 | -14.327 | 19.162 |
| -22.411 | 37.538 | -16.164 | 21.325 |
| -20.572 | 35.857 | -18.002 | 23.341 |
| -18.736 | 33.829 | -19.839 | 25.226 |
| -16.899 | 31.472 | -21.675 | 26.895 |
| -15.062 | 28.736 | -23.512 | 28.221 |
| -13.226 | 25.685 | -25.349 | 29.226 |
| -13.891 | 22.444 | -27.185 | 29.971 |
| -09.552 | 18.908 | -29.022 | 30.484 |
| -07.714 | 15.314 | -30.860 | 30.787 |
| -05.877 | 11.348 | -32.697 | 30.920 |
| -04.041 | 07.042 | -34.372 | 30.894 |
| -02.204 | 02.307 | - | - |

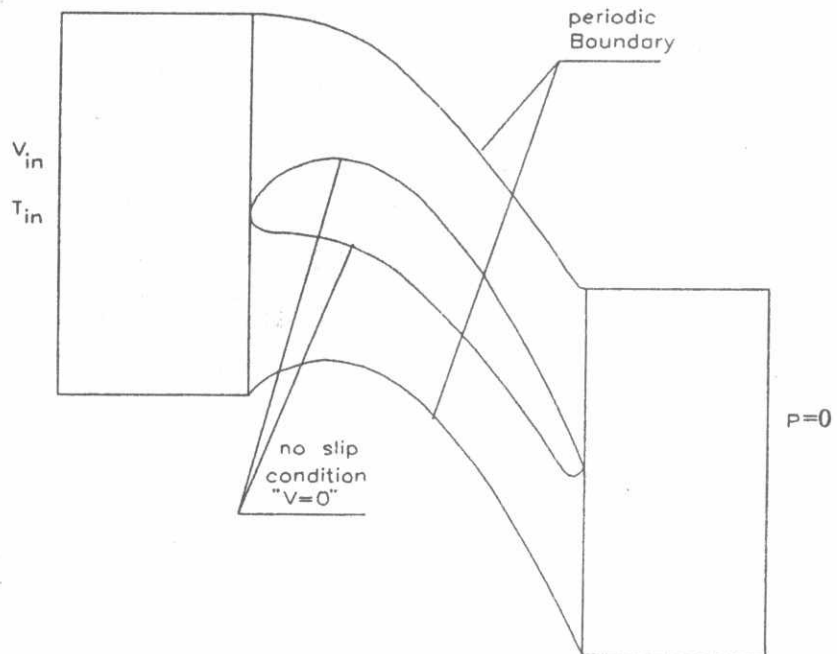


Fig. 1. Fluid flow boundary conditions

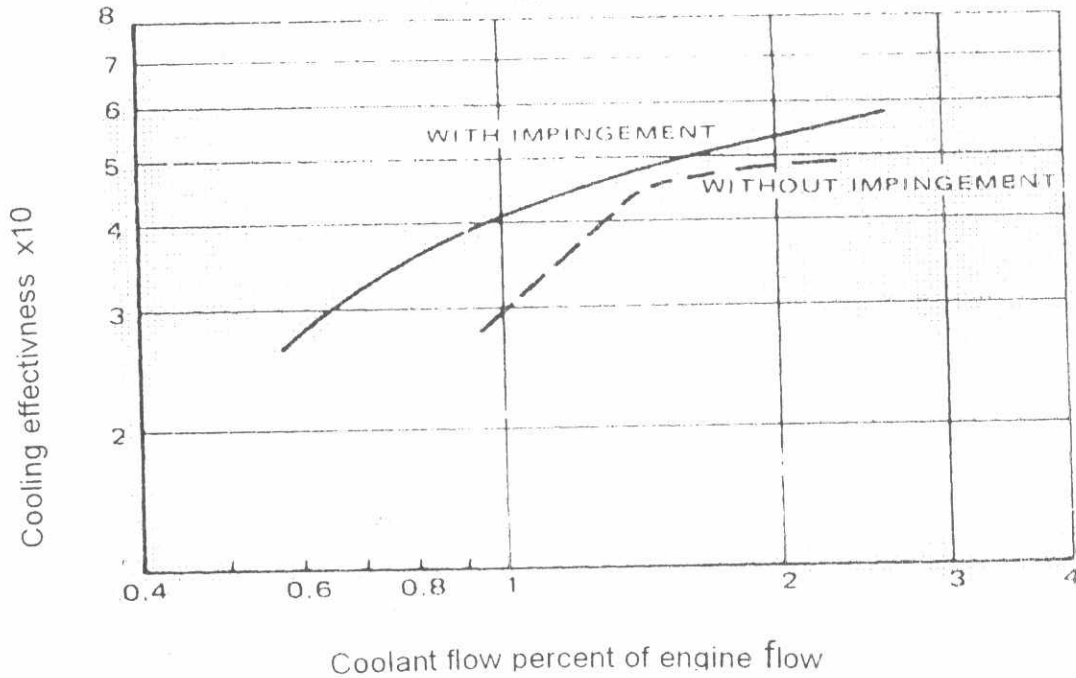


Fig. 2. Cooling effectiveness of convective cooling conditions

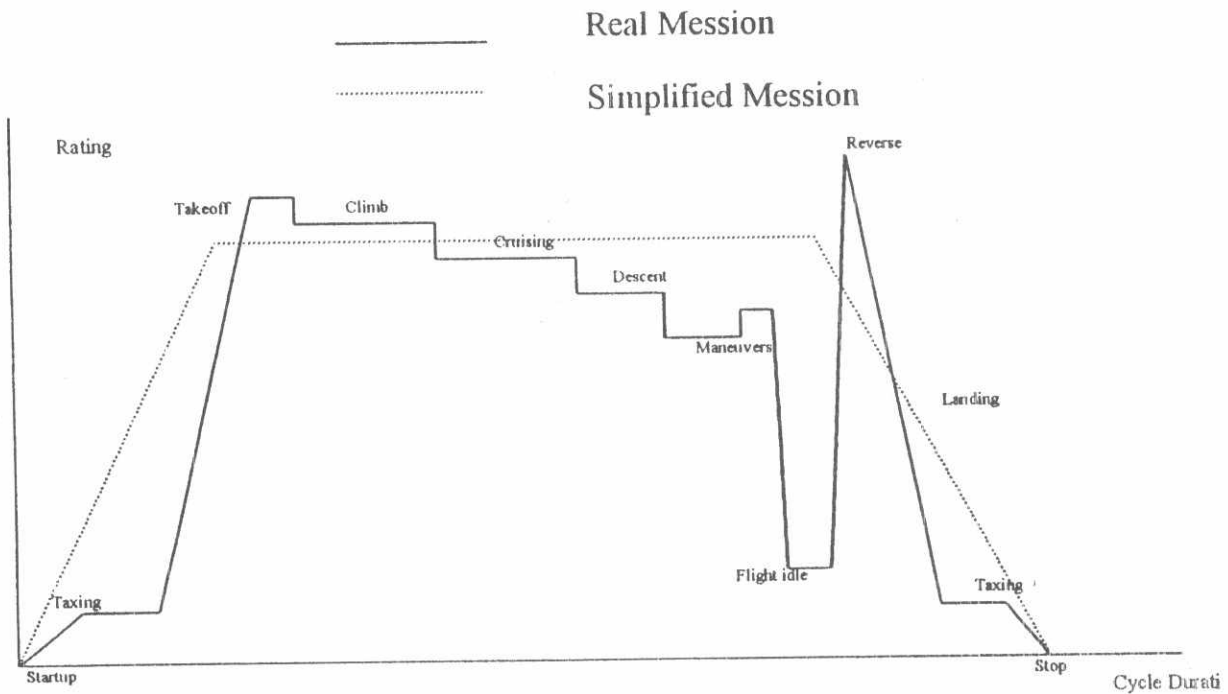


Fig. 3. Real and Simplified Mission Cycle

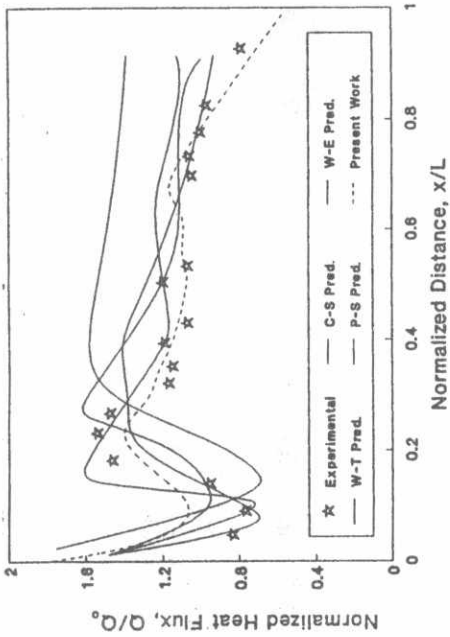


Fig. 6. Suction side heat flux distribution

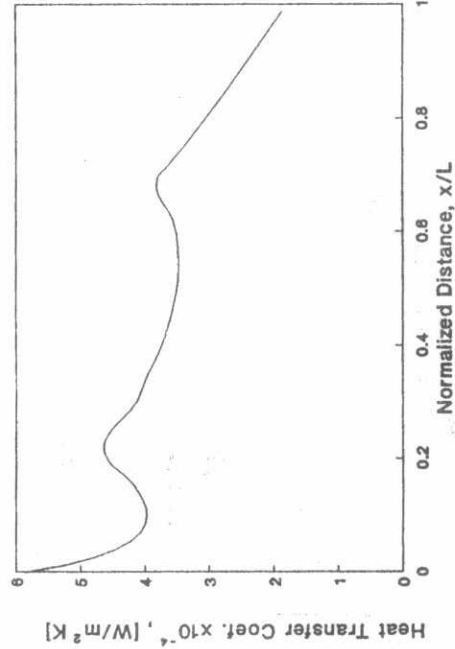


Fig. 7. Suction side heat transfer coefficient distribution

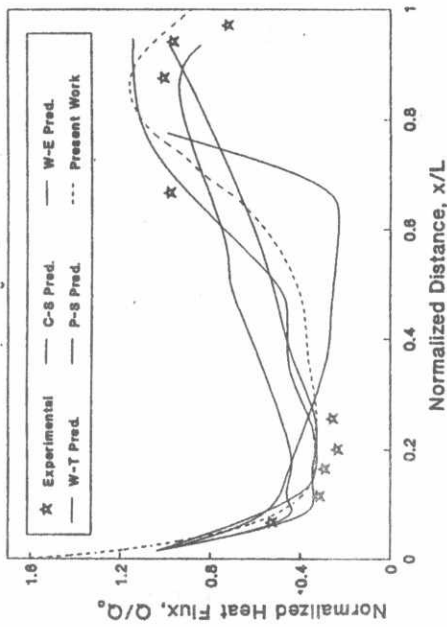


Fig. 4. Pressure side heat flux distribution

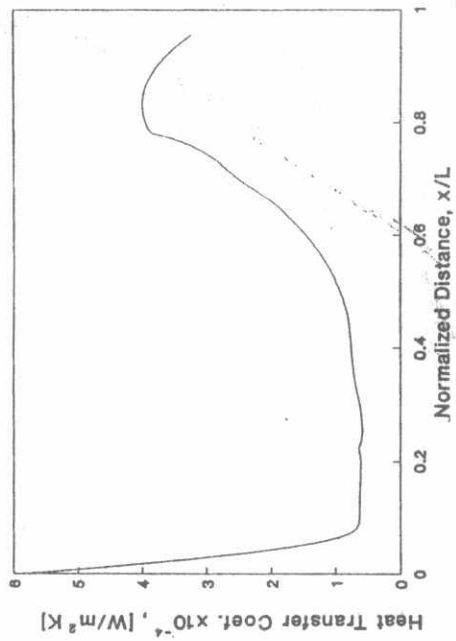


Fig. 5. Pressure side heat transfer coefficient distribution

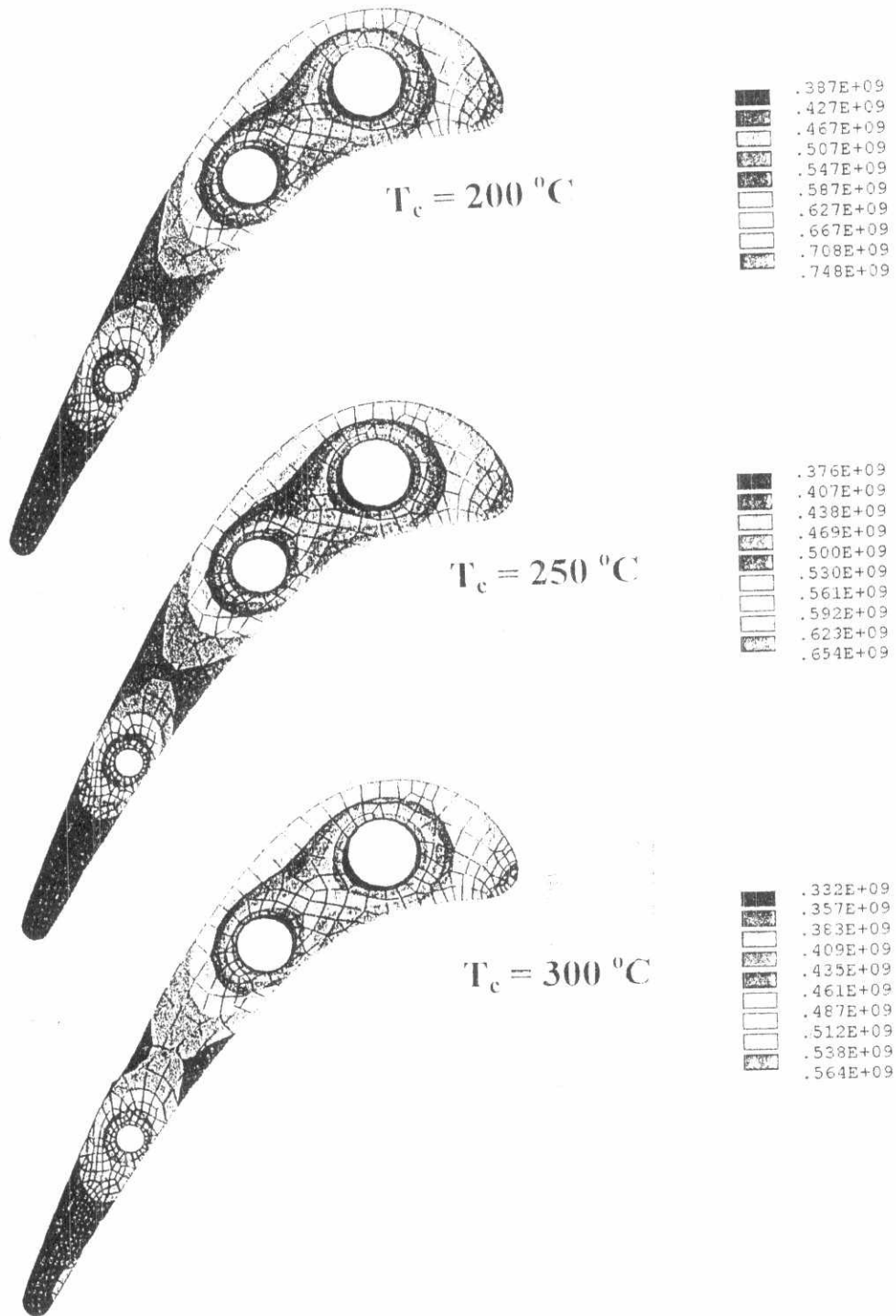


Fig. 8. Effect of cooling air temperature on the stress distribution

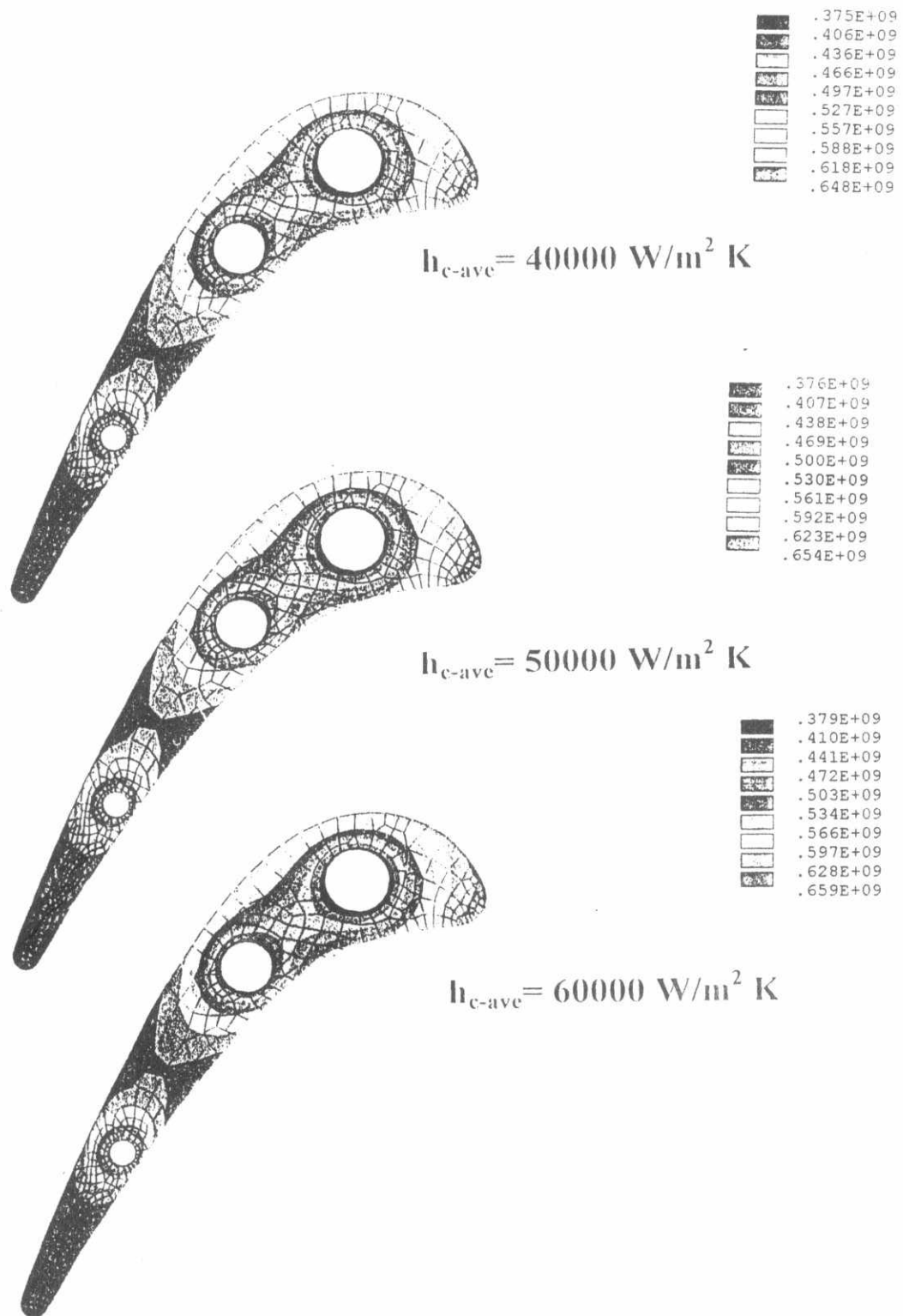


Fig. 9. Effect of cooling passages heat transfer coefficients on the stress distribution